Original scientific papers UDK 620.91:514.12
doi: 10.7251/COMEN1502193M

MATERIALS SCIENCE AND ENERGY FRACTAL NATURE NEW FRONTIERS

Vojislav V. Mitić[1,2,], Hans-Jörg Fecht[3], Ljubiša M. Kocić[1]*

[1] Faculty of Electronic Engineering, University of Niš, Aleksandra Medvedeva 16, Niš, Serbia
[2] Institute of Technical Sciences of the Serbian Academy of Sciences and Arts
[3]Institute of Micro and Nanomaterials University of Ulm, 89081 Ulm, Germany

Abstract: The modern material science faces very important priorities of the future new frontiers which open new directions within higher and deeper structure knowledge even down to nano and due to the lack of energy, towards new and alternative energy sources. For example, in our up to date research we have recognized that BaTiO3 and other ceramics have fractal configuration nature based on three different phenomena. First, ceramic grains have fractal shape looking as a contour in cross section or as a surface. Second, there is the so-called "negative space" made of pores and inter-granular space. Being extremely complex, the pore space plays an important role in microelectronics, micro-capacity, PTC, piezoelectric and other phenomena. Third, there is a Brownian process of fractal motions inside the material during and after sintering in the form of micro-particles flow: ions, atoms and electrons. Here we met an exciting task of the Coble model, with already extended and generalized geometries. These triple factors, in combination, make the microelectronic environment of very peculiar electro-static/dynamic combination. The stress is here set on inter-granular micro-capacity and super micro-capacitors in function of higher energy harvesting and energy storage. An attention is paid to components affecting overall impedances distribution. Constructive fractal theory allows recognizing micro-capacitors with fractal electrodes. The method is based on the iterative process of interpolation which is compatible with the model of grains itself. Inter-granular permeability is taken as a function of temperature as fundamental thermodynamic parameter.

Keywords: $BaTiO_3$-ceramics, fractals, microstructure, micro-impedances.

1. INTRODUCTION

Barium-titanate ceramics is one of the most important electronic ceramics for the small size and multilayer capacitors of high capacitance manufacture. For these applications this ferroelectric is usually doped with various additives such as Er^{+}, Ho^{3+}, Mn^{2+}, Nb^{5+}, Zr^{2+}, Yb^{3+}, and some oxides, in an attempt to achieve temperature-stable dielectrics. It is shown that dielectric constant depends strongly on grain and pore size in the ferroelectric state, i.e. the finer the grain size, the higher the dielectric constant. The investigation of microstructure characteristics of undoped and doped $BaTiO_3$ in the function of consolidation parameters is a necessary step in barium-titanate ceramics processing and designing. Structure investigations provide better understanding of dialectic properties, especially from the point of view of the relative dielectric constant response of pure and doped $BaTiO_3$-ceramics. Fractal method traces a new approach for describing and modelling the grain's shape and relations between $BaTiO_3$-ceramics structure and electrical properties. It gives more natural approximation to the grain's boundary, whereas the construction uses recursive random algorithms. Particle shape is a fundamental powder property, affecting powder packing and thus bulk density, porosity, permeability, cohesion, flowability, attrition, interaction with fluids, covering ability of pigments, resistance, capacity, magnetic permeability etc. Introducing mathematically well-established fractal nature theory in the powder metallurgy science, new materials, nano-technology, „free-floating" metallic drops processing, various ceramics technologies, graphene oxide flakes, literally from trash recycling to self-healing materials, become more complete explained and connected.

Using the fractal theory modern developments, offers enough firm arguments to support modelling,

* Corresponding author: vmitic.d2480@gmail.com

predicting and many modern technological processes control, as outstanding examples of fractal-based structures. Estimation of the fractal analysis main parameter − the Hausdorff or fractal dimension, for all relevant morphologies that appear in consolidation processes is of crucial importance. By using obtained values, the study of their impacts on distribution of energy, temperature, surface tension, dielectric constants, rate of densification etc., can be performed. The fractal analysis is used in ceramics materials to quantify the particle's structure complexity, granular complexes, sintering processes, pores distribution changes etc. (For some other ceramics samples the pressure is up to 150 MPa).

2. EXPERIMENTAL PROCEDURE

In this paper, Er_2O_3, Yb_2O_3, Ho_2O_3, Mn_2O_3, Nb_2O_3, doped $BaTiO_3$-ceramics were used for microstructure characterization and modelling. The samples were prepared from high purity (>99.98%) commercial $BaTiO_3$ powder (MURATA) with [Ba]/[Ti]=1,005 and Ho_2O_3 powders (Fluka chemika) by conventional solid state sintering procedure. The content of Ho_2O_3 ranged from 0.50 to 2.0 wt%. After drying at 200 ºC for several hours, the powders were pressed into disk of 7mm in diameter and 3mm in thickness under 120 MPa. The compacts were sintered from 1320ºC to 1380ºC in air for four hours. The microstructures of sintered and chemically etched samples were observed by scanning electron microscope (JEOL-JSM 5300) equipped with energy dispersive spectrometer (EDS-QX 2000S).

3. BASIC WORK, EXPERIMENTS AND RESULTS

The first results of joint work of the group guided by prof. Mitić and Kocić appeared around the mid-90s of the last century. All was based on a strict mathematical treatment of approximated ceramics micro-morphology and using more advanced and even daring approaches including the first usage of fractals as a tool in the systematic ceramics studying and similar materials.

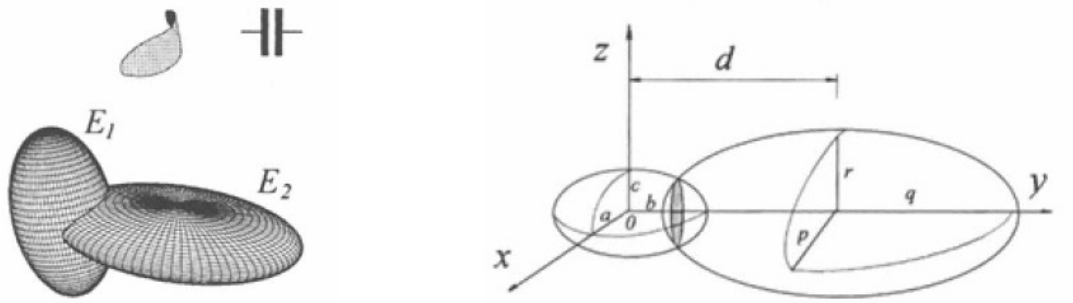

Figure 1. Left. Ellipsoidal model of the grain's contacts and formation of inter-grain micro capacitor. Right. Contact geometry

Here, the result from 1998 [1] that generalizes Coble's model of two grains in contact are presented. Instead of two equiradial spheres, two ellipsoids E_1 and E_2 (Figure 1) are considered with different dimensions. Different models were studied assuming that one or both grains belong to one of three approximate classes: polyhedrons or prisms (P), spheres (S) or ellipsoids (including spheroids) (E). All possible two-grain contact combinations have been considered: P-P, S-S, E-E, P-S, P-E and S-E [10−12].

The contact zone, shown in the left figure has an approximate shape as indicated above and may be considered as a micro-capacitor. In the case of coaxial ellipsoids, having proportional parallel semi axes, the surface of the ellipse is made in the intersection of two surfaces. Indeed, if the parallel semi-axes are *a*, *c* and *p*, *q* obey the proportional relation

$$\frac{p}{a}=\frac{r}{c},$$

then the common elliptic disk area is given by

$$S=\pi ac\left(1-\left(\alpha d-\beta\sqrt{\gamma+d^2}\right)^2\right),$$

where *d* is ellipsoids' centres distance and

$$\alpha=\frac{k^2q}{k^2b^2-q^2},\ \beta=\frac{k^2q}{k^2b^2-q^2},\ \gamma=\left(1-\frac{1}{k^2}\right)\left(k^2b^2-q^2\right).$$

The functional diagrams *S*(*d*) are shown in the above figure. Three different diagrams correlate to proportion ratios and the third semi-axis length.

In the same year, the paper [2] was published with further elaboration of the idea of ellipsoidal approximation of grains being randomly scattered

through the space, making a kind of firm packing but still with a substantial quantity of pores. Using the set-theory characteristic function

$$\chi_A(x) = \begin{cases} 1, & x \in A \\ 0, \text{ otherwise}, \end{cases}$$

applied on the grains' clusters to describe their different morphologies, like these shown in Figure 2.

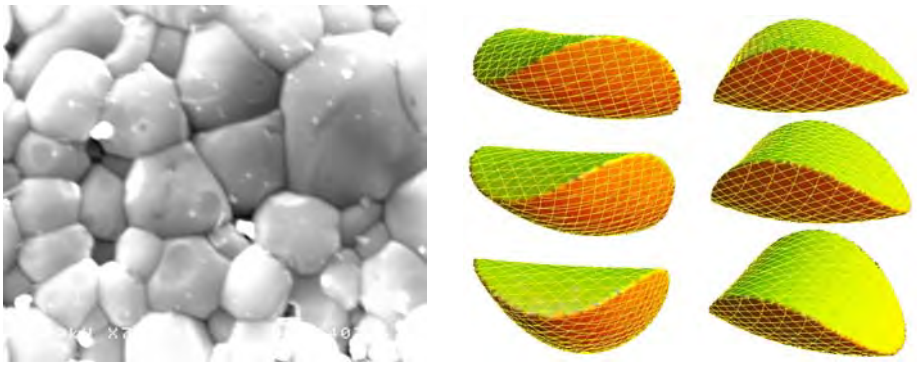

Figure 2. The real $BaTiO_3$ grains (left) and the computer models of common, intergranular zones of ellipsoidal modelled inter-grain surfaces (right)

Now, define

$$F(\vec{r}) = \sum_{i \in I} \chi_{G_i}(\vec{r}),$$

the function F, being discontinuous at the surface points of these zones. The shape and size of intergranular domains shown in Figure 2 (on the right) is responsible for integral micro-capacity, and is explained by function F. On the other hand, the quality of the surface of these domains, its roughness and unevenness increases the possibility of establishing new micro-contacts which directly increases integral capacity of the inter-grain domains. So, in the same paper [2], the first estimation of the fractal dimension of the grains contours is given. It was $DH_f = 1.0677699$. The method being used for this first attempt is the box-counting method based on the famous formula

$$DH_f = \lim_{r \to 0} \frac{\ln N(r)}{\ln(1/r)} \qquad (1)$$

where $N(r)$ denotes the number of boxes (square boxes in 2*D* space or cubits in 3*D* space) which characterizes the so-called „slim" fractal, i.e. the fractal that is quite close to the smooth contour.

Let *M* be the measure of the object *S* characterized by *length*, *area*, *volume* (or hyper-volume), but also by *mass*, *charge of electricity*, etc. At the same time, let *l* be the linear dimension of *S*, like length, thickness or diameter. Then, for *S* being classical, Euclidean object, immerged in the space of dimension (also called *topological dimension*) D_T, the *power law* takes place

$$M(l) \propto l^{D_T}. \qquad (2)$$

The role of proportionality constant in (2), plays the D_T-dimensional *density* $\rho = \rho(l)$. By definition,

$$\rho(l) = M(l) \times l^{-D_T}. \qquad (3)$$

So, for d = 1, 2 and 3, the relation (3) may represent *mass density*, *particle density*, *electric charge density*, *energy density* etc.

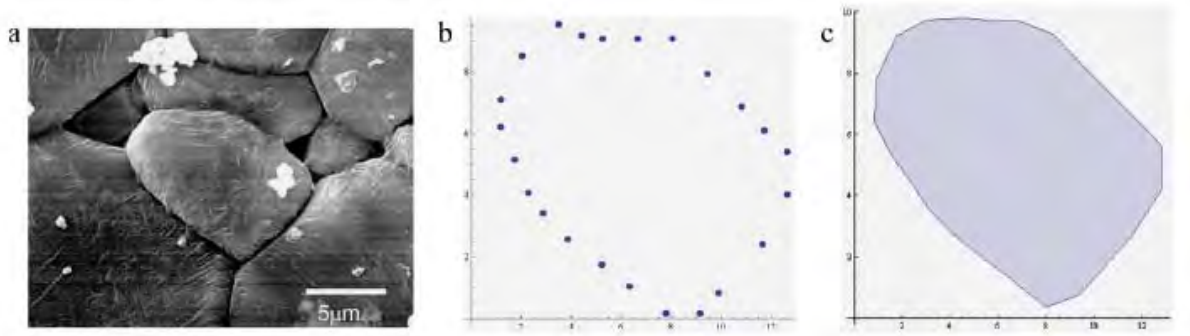

Figure 3. Left. The grain contour extraction from SEM photo

Now, for fractal object *S*, characterized by fractal dimension DH_f that always strictly exceeds topological dimension $DH_f > D_T$, it holds $M(l) = Const \times l^{-D_T}$, so that

$$\rho(l)=\frac{M(l)}{l^{D_T}}=\text{Const}\times\frac{l^{DH_f}}{l^{D_T}}=\text{Const}\times l^{DH_f-D_T}. \quad (4)$$

The formula (4) is very useful in estimation of fractal dimension of some fractal objects. If, for example, one needs to know an approximate fractal dimension of the micro-particle's contour, the role of $\rho(l)$ plays the length of the contour L as a function of the accepted unit of measure δ, so, $L(\delta)$ and, taking into account that the contour is a one-dimensional object ($D_T=1$), one gets

$$L(\delta)=\text{Const}\times\delta^{1-DH_f}$$

which is called *Richardson law*, (also, *Mandelbrot-Richardson law*). By taking logarithm (any base), and for a series of measures with (typically) decreasing sequence of etalon measures $\{\delta_k;\ k=1,2,...,n\}$, $\delta_{k+1}<\delta_k$, the linear relationship emanates

$$\log L(\delta_k)=DH_f\log\delta_k+\text{Const} \quad (5)$$

in the $(\log\delta,\log L(\delta))$ coordinate system. The procedure requires fitting the line through the data $(\log\delta_k,\log L(\delta_k))$ to find its slope coefficient DH_f. An example applied on the Koch snowflake curve shown in Figure 4, reveals using square mesh with „cells" sides δ_k, decreasing in the manner of geometric sequence by choosing $\delta_{k+1}=\frac{1}{2}\delta_k$. The log-log diagram presented in Figure 7 (on the left) gives DH_f = 1.258 as the calculated value. The theoretic value for Koch snowflake is DH_f = 1.2619.

Figure 5 (on the right) shows dependence of approximation error of the choice of metrics being used for the least square fitting procedure. Namely, if the distance between two plane points having coordinates $(x_i,\ y_i)$ and $(x_j,\ y_j)$ be defined using generalized *p*-norm

$$\text{dist}_p\left((x_i,\ y_i),\left(x_j,\ y_j\right)\right)=\left(\left|x_i-x_j\right|^p+\left|y_i-y_j\right|^p\right)^{1/p},\ p>1,$$

depending on the parameter $1<p<+\infty$. For $p=2$, the above metric reduces on the usual Euclidean distance, and Figure 5 (on the right) shows the circle as a set of points (in the plane) having constant distance from the point *M*, and therefore, the closest point on the line is the tangent point M_2. As *p* increases in the interval $[2,+\infty)$, the point M_2 moves towards $M_{+\infty}$, which is the closest point on the line to *M*, in $p\to+\infty$ metrics. On the other hand, M_1 is the closest in *p* = 1 metrics.

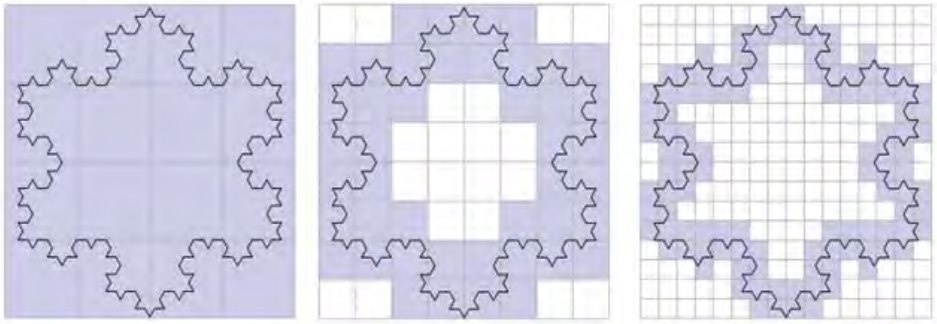

Figure 4. Successive halving of box side length results in decreasing sequence of covers

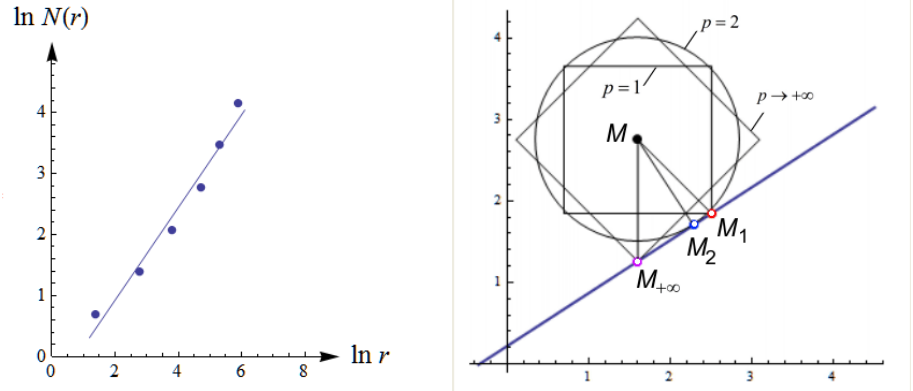

Figure 5. Left. The log-log fitting diagram for extracted Box-counting data. Right. The possible error source in generalized l_p metrics

Applied to pure $BaTiO_3$ or with various additives (Er^{+}, Ho^{3+}, Mn^{2+}, Nb^{5+}, Zr^{2+}, Yb^{3+}), and some oxides, and similar perovskite ceramics, a grain contour line fractal dimension has relatively small values [9,10,15,16]

$1.02 < DH_f$ (contour) < 1.30,

which is quite in agreement with other author's results (see Smirnov [11], p.38). For the grains' surface, according to our experiments, the fractal dimension satisfies [12],

$2.01 < DH_f$ (grain's surface) < 2.095.

It is natural that DH_f values both for grains' contours or surfaces depend on the ceramics sintering phase, additives concentration and technological parameters (temperature, pressure, duration). Further investigations paid attention to the SEM photos of the surface of ceramics materials, looking as the two dimensional pattern. The estimation yields [16]

$1.60 < DH_f$ (surface of specimen) < 1.90.

The grains as solitary objects are electrical micro accumulators and therefore the sources of electrical potential energy and integral capacitors. The known rule gives the potential energy of a solitary grain being on the time dependent potential difference (voltage) $v(t)$, and bearing the quantity of electricity $q(t)$ to be

$$E_{grain}(t) = \frac{1}{2} q(t) v(t) . \qquad (6)$$

This relation is very important as it gives the energy stored in the body of every individual grain, with time dependency. The structure of the grain also has its volume fractality which seems to be still unknown, but very close to 3.

From the energetic point of view, it is important, besides the grains themselves, to study intergranular morphology, especially in the context of fractals.

4. FRACTALITY AND CERAMICS GRAINS' CONTACTS

Electronics ceramics, especially $BaTiO_3$-ceramics, are made out of very fine powder having the maximum Ferret diameter. These particles have such a high surface energy to fuse together and to make sintered ceramics. As it is well known [1−10], many powder materials have fractal structure, and nowadays it is a well established, documented and widely accepted fact. Fractal geometry, systematically introduced by Benoit Mandelbrot [3,4] at the end of the sixth and the beginning of the seventh decade of the last century (for a constructive approach, see Barnsley [5]) as an efficient toll for describing complex non-Euclidean shapes.

Consider a structural pattern of three sphere-shaped ceramic grains, contacting each other in only one point and making pointwise contacts (Figure 6, left). By decreasing the distance between centres of these spheres the body of each sphere sinks into another one, forming a virtual body as in Figure 2, on the right. Once that we have a method of retrieving the fractal dimension, we get a chance to go deeper into the nature of micro grain contacts. At this point the concept of *generalized Minkowski hull* comes forward. The associated with a plane contour *G*, and generated by a convex plane figure *S*, sliding along *G* in the manner that one fixed point of *S* coincide with one *G* point. The concept of Minkowski hull is very useful in explanation of the contact zones nature.

The union of all points of *S* made by covering the whole way back to the starting point is a two-dimensional layer called *generalized Minkowski hull.* It is shown in Figure 6, on the right.

Let r_1 and r_2 be minimal and respectively maximal Ferret diameter of *S*.

$$r_1 = \min \operatorname{diam}(S), \quad r_2 = \max \operatorname{diam}(S),$$

The generalized Minkowski hull's thickness $\rho(\theta)$ is the function of polar angle θ, with respect to the pole that may be fixed at, for example, centroid of *S*.

Consider two grains, *A* and *B* with hulls having variable thickness r_A and r_B, respectively

$$r_A = \min_{0<\theta<2\pi} \rho_A(\theta), \quad r_B = \min_{0<\theta<2\pi} \rho_B(\theta) .$$

The meaning of these distances and the generalized Minkowski hulls is that the grains' coarseness stays inside the hull. It means that no micro relief hills overtop the hull boundary. If two grains are in a position when their distance *d* is not bigger than the sum $r_A + r_B$, the grains are in the *position of the first touch.*

If *d* becomes smaller than $r_A + r_B$, the intergranular zone appears.

The second characteristic position is when the either hull's contour touches the other grain's body, i.e., when $d = \max\{ r_A, r_B \}$, the *second contact* is encountered. The *third contact* comes when $d = \min\{ r_A, r_B \}$. The contact of two grains in only one point is the fourth contact, in two points is the *fifth contact* and, finally if 3 points are common, it is the sixth contact.

Without the concept of fractal surface, the above considerations will be pointless.

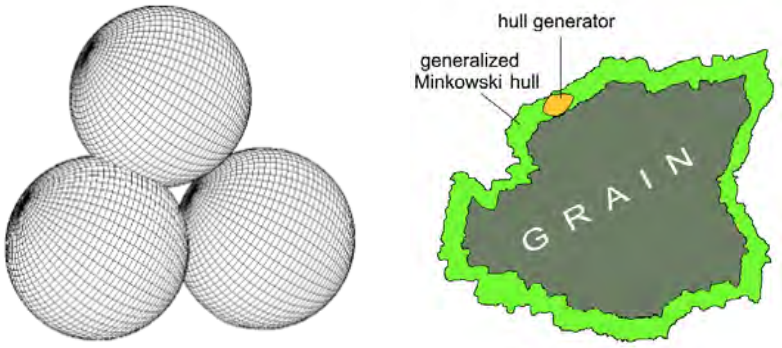

Figure 6. Left. Forming the intergrain zone in the case of three spherical grains Right. The real grain and its generalized Minkovski hull

Figures 7 and 8 describe 3D reconstruction of the real shapes of ceramics grains. Figure 7 also contains the box-counting procedure with application of grey-shade algorithm, which extracts the fractal dimension of the ceramics surface that is substantially bigger than the dimension of the individual grain.

Shapes which are not fractal are the exception, said Mandelbrot. The fractal geometry key concept is the unique number that is connected with the fractal object which is known as *fractal dimension*, a concept introduced sixty years ago by Felix Hausdorff. If DH_f denotes fractal dimension, the simple inequality $DH_f > DT$, where DT is topological dimension, has been suggested by Mandelbrot as an acceptable (although not complete) definition of fractal objects.

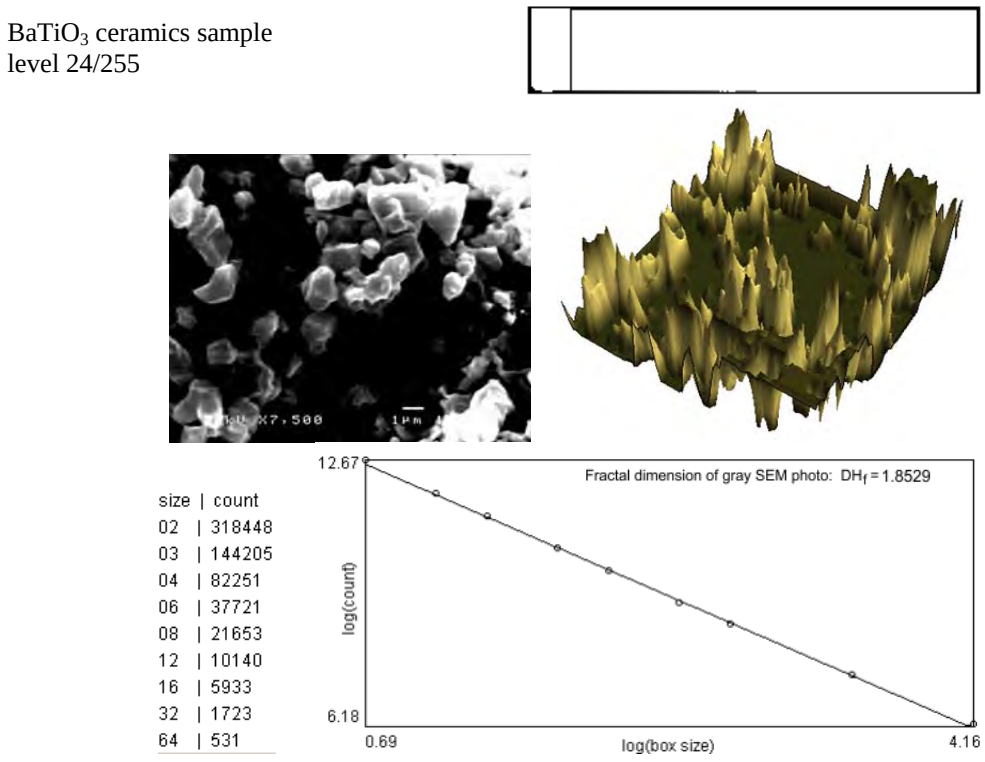

Figure 7. Fractal dimension estimation using grey shades box counting algorithm applied at the SEM photograph in the middle, left part. In the middle, on the right is the reconstruction of the surface as a 3D object. The value estimated is $DH_f = 1.8529$. The data and log-log diagram are shown below

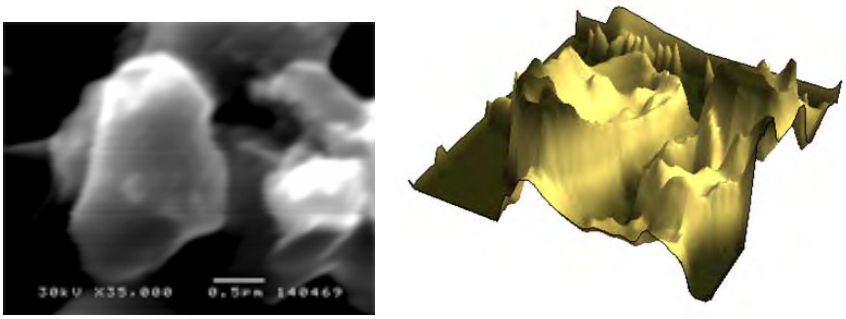

Figure 8. Two $BaTiO_3$ grain's in contact and 3D reconstruction

If two grains are in contact as shown in the SEM in Figure 8, a huge set of spots may be encountered as potential contact sites. The good candidates are the exposed points at each grain, but also flat areas where gradient of the function describing grain's surface is locally constant, or, $\nabla g = [\partial g/\partial x \;\; \partial g/\partial y \;\; \partial g/\partial z]^{\mathrm{T}} = \mathrm{Const.}$ Such spots are shown on the surface in Figure 9, as locally flat rectangles or squares having maximal diameter approximately of the magnitude $10^{-2} \times \mathrm{diam}(S)$.

Another means of the analysis that reveals a heavy disorder contact surfaces and confirm their fractality is discrete Fourier analysis. For discrete cosine (DCT), the following four representations are known

$$a)\quad dct_1(u) = \sqrt{\frac{2}{n-1}}\left(\frac{u_1}{2} + \sum_{r=2}^{n-1} u_r \cos\left(\frac{\pi}{n-1}(r-1)(s-1)\right) + (-1)^{s-1}\frac{u_n}{2}\right),$$

$$b)\quad dct_2(u) = \frac{1}{\sqrt{n}}\sum_{r=1}^{n} u_r \cos\left(\frac{\pi}{n}\left(r-\frac{1}{2}\right)(s-1)\right),$$

$$c)\quad dct_3(u) = \frac{1}{\sqrt{n}}\left(u_1 + 2\sum_{r=2}^{n} u_r \cos\left(\frac{\pi}{n}(r-1)\left(s-\frac{1}{2}\right)\right)\right),$$

and

$$d)\quad dct_4(u) = \sqrt{\frac{2}{n}}\left(\sum_{r=1}^{n} u_r \cos\left(\frac{\pi}{n}\left(r-\frac{1}{2}\right)\left(s-\frac{1}{2}\right)\right)\right).$$

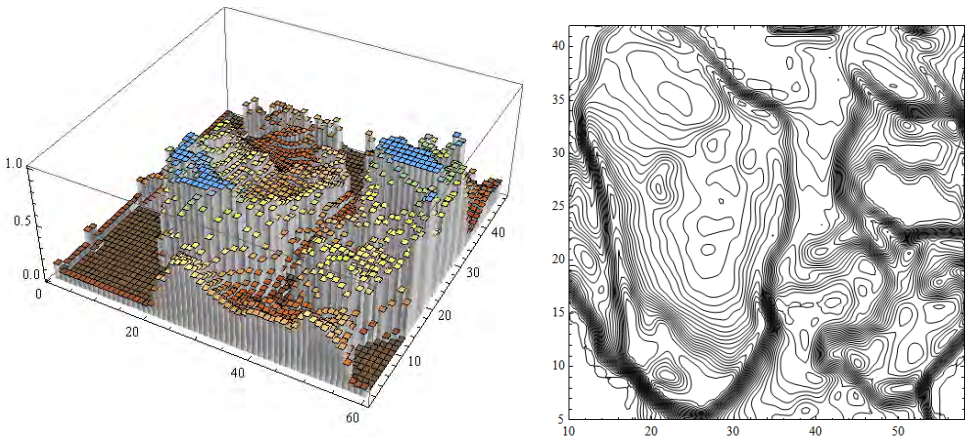

Figure 9. Left. Possible contacting spots for the grains from Figure 10. Right. Smoothing the piecewise constant function from the left, the grains' shapes can be retrieved

The corresponding graphs showing the absolute value of diagonal elements of the discretized surface data array *u* (Figure 10).

Using the Mandelbrot's formula that gives a relationship between the length *L* of a fractal "space filling" curve of fractal dimension DH_f that "fills" the two-dimensional area of size *A* , i.e.,

$$L^{-DH_f} = K\sqrt{A}, \quad (K \text{ is constant}),$$

in combination with Richardson law of variable yardstick, upon which a fractal curve length depends on measurement precision, i.e. on the measure yardstick length δ is

$$L = \delta^{1-DH_f},$$

gives A as a function of DH_f

$$A(DH_f) = K\,\delta^{2\left(\frac{1}{DH_f}-1\right)}.$$

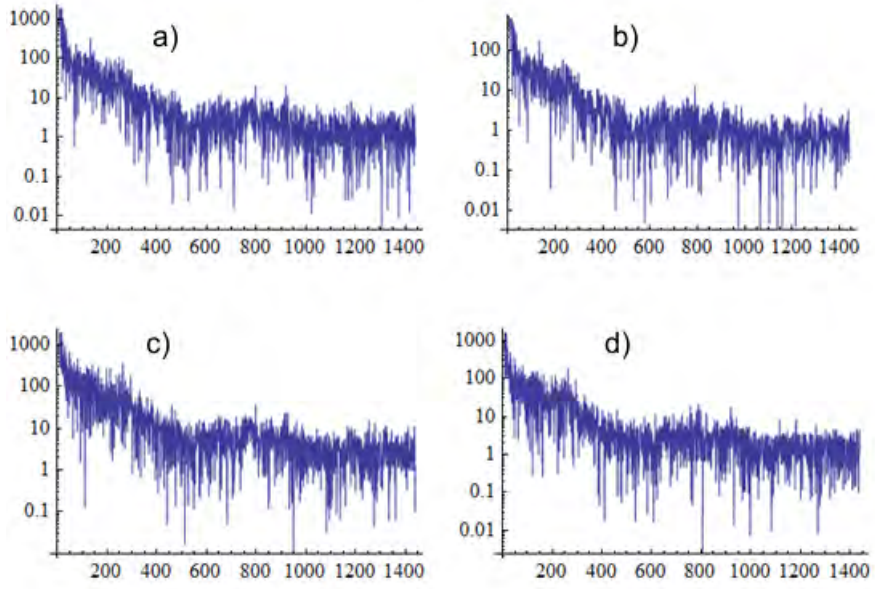

Figure 10. Four types of Discrete Cosine Transform (DCT) reveal main and secondary harmonics having configuration typical for fractal surfaces

The physical meaning of the last equation is the functional dependence of the capacitor electrode area size with fractal dimension DH_f that can be measured using different algorithms, as explained above.

Such considerations did help in gaining the approximate value of neck cross section area size A in Coble two grain contact model, where real cross section is approximated by a, b semi-axes elliptic disc as

$$A_{\text{Coble}} = 2ab\pi\,\delta^{2\left(\frac{1}{DH_f}-1\right)}.$$

It is clear from the last two formulas that the surface area increases when δ gets smaller; theoretically, for $1 < DH_f$, $A \to +\infty$ when $\delta \to 0_+$.

In addition, the area of ceramics surface (as a cluster of grains) as well as the area of a single grain surface, depends on the unit of measure δ and local fractal dimension DH_f and is given by ([25])

$$A(\delta,\ DH_f) \sim \delta^{2-DH_f}. \qquad (7)$$

The relationship (7) is illustrated by the graphs in Figure 11. The increasing of the contact area size with more precise measuring (smaller d) is evident for all fractal dimensions > 2. Even for „smooth“ fractal surfaces, i.e. surfaces with DH_f close to 2 (as it is the case with $BaTiO_3$-ceramics grains surfaces having $2.079 < DH_f < 2.095$), the area size A duplicates its value if the unit of measure d decreases by the factor 2.87389×10^{-4}.

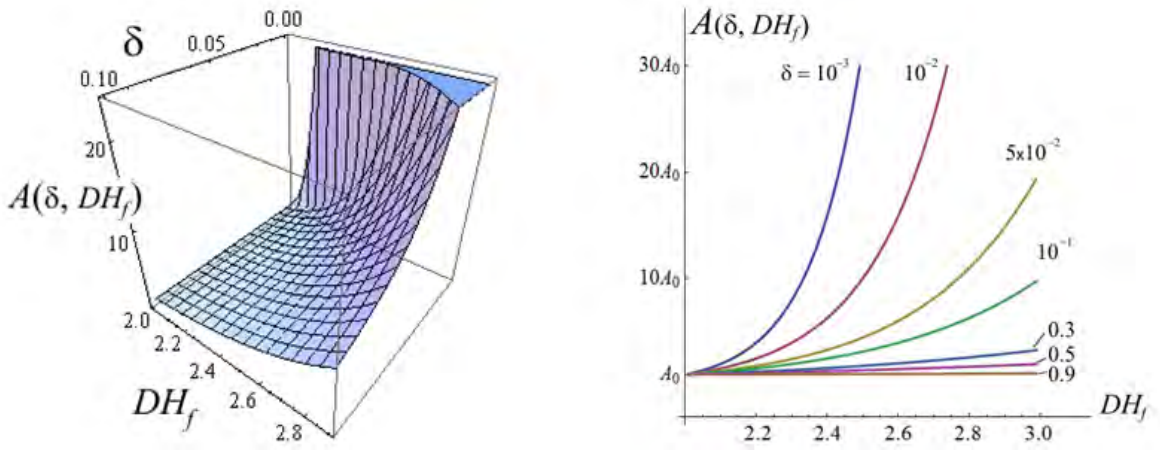

Figure 11. Size of the contact area $A(\delta, DH_f)$ vs. fractal dimension. A0 in the right 2D graph is the area size for ideally flat contact surface

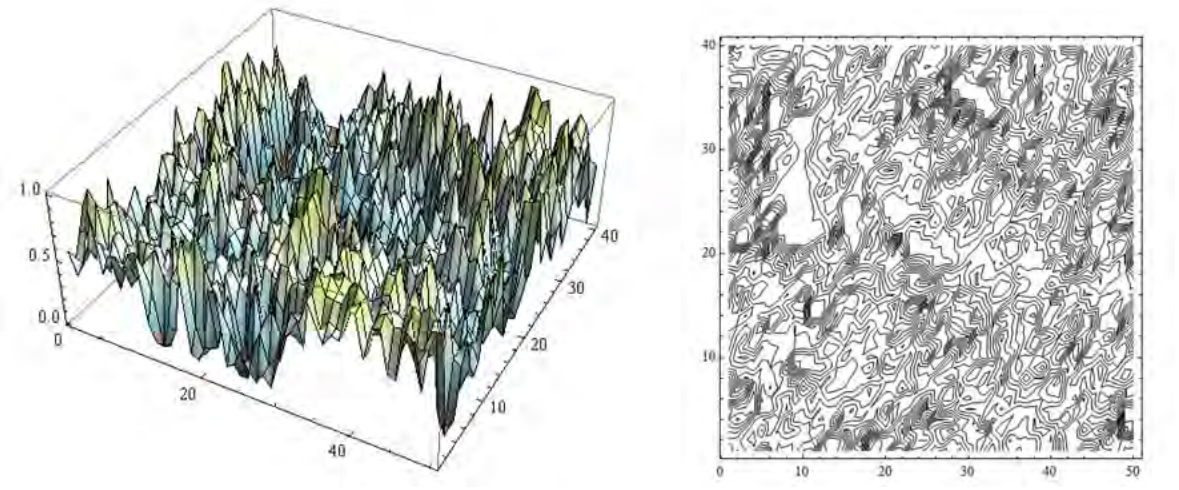

Figure 12. Left. Reconstruction of 3D-surface for BaTiO3 sample; Right. Level lines of the same surface. Picks represent grains. The similarity with Earth relief iso-lines is obvious

While the fractal dimension of $BaTiO_3$-ceramics grain's surface is modest, the dimension of the specimen surface is much higher, as shown in Figure 11. The fractal dimension is calculated using max-gray level box-counting method of the SEM, which gives DH_f = 1.7531. For other specimens similar values are obtained in the range from 1.7529 to 1.8025.

These results led to revision of the formula for parallel-plate capacitor with plates area size A and a separation d ($d << A^{1/2}$)

$$C = \varepsilon_r \varepsilon_0 \frac{A}{d},$$

where e_r and e_0 are dielectric constants of $BaTiO_3$-ceramics grains contact zone and in vacuum respectively. Namely, the intergranular micro capacitor, formed in the contact zone of two ceramics grains is *not* a parallel-plate capacitor. It is a fractal capacitor that may be thought of as being a product of an iterative process described in Figure 13, left. The top subfigure shows a parallel-plate capacitor as described above. It corresponds to a capacitor (denoted by C_0) with adjacent grains' perfectly flat contact surfaces which do not exist in reality. On the contrary, the contact surface is rough and uneven, so that the following fractal model will be a good approximation. Suppose that the flat parallel geometry of C_0 (Figure 13, left) is replaced by three flat capacitors „Z"-shaped configuration connected in parallel, forming the unique capacitor C_1.

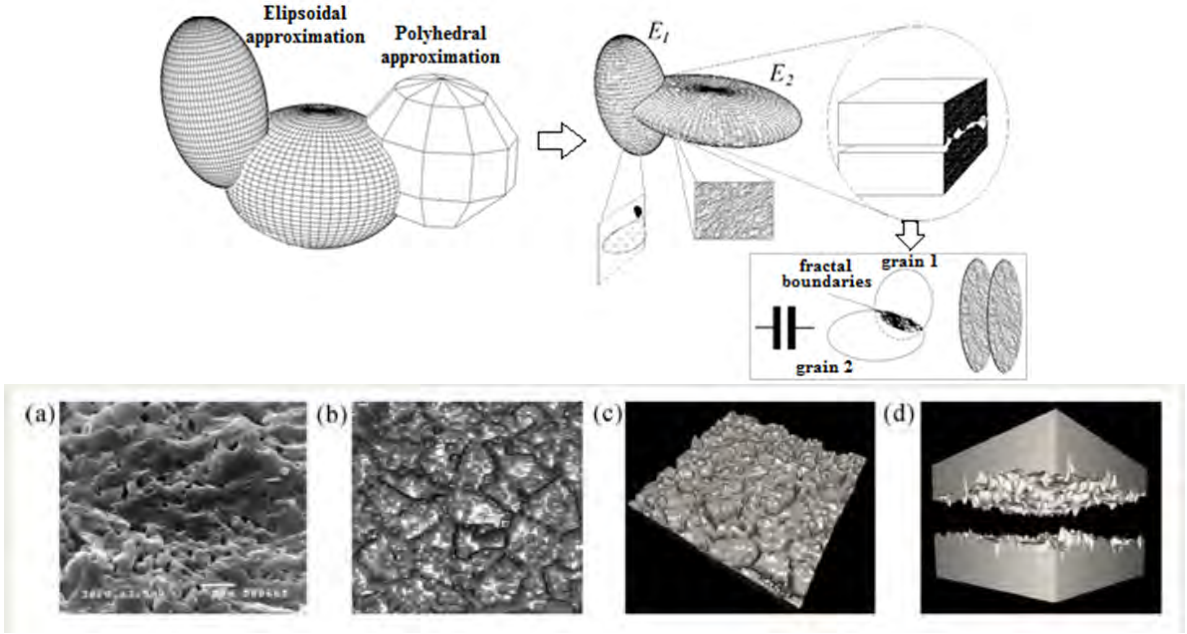

Figure 13. Above. Grain contacts: From ideal Euclidean shapes and contacts to real, fractal-like capacitor electrode forms. Below. SEM shots and computer reconstruction of rough contact surfaces

In the next stage, each of three linear segments is replaced by another smaller „Z“ made out of three smaller flat capacitors. By continuing this procedure, the sequence of more and more segmented chains of sub-capacitors C_0, C_1 , C_2,..., is obtained (Figure 5, on the right). It is suitable to take each smaller „Z“ to be a shrunk *affine image* of the bigger „Z“ standing in the above line. In this manner, the separating distance would be shrunk as well for some factor (although it is not shown in our figure for clarity reasons). This factor (called vertical scaling factor), makes the ratio $d/\sqrt{A}$ smaller for each iteration, making capacity to increase. Also, the sum of the lengths in each iteration increases due to the wiggling form of the higher stage capacitor. In all, the capacity of C_n will be substantially higher than C_0. This increment is characterized by the ratio $\alpha_0 = \lim_{n\to\infty} C_n / C_0$ and thus, if C_f stands for "fractal capacitor"

$$C_f = \lim_{n\to\infty} C_n = \alpha_0 \varepsilon_r \varepsilon_0 \frac{A}{d} = \alpha_0 \left(\varepsilon_r \varepsilon_0 \frac{A}{d} \right) = \alpha_0 C \qquad (8)$$

where C is the capacity of the capacitor having ideally flat plates. Since $C_f > C$, it follows that $\alpha_0 > 1$. This effect of increasing capacity due to fractality of the contact zone is referred to by these authors as the α-correction of the intergranular capacity or, which is the same, dielectric constant, by stating $\varepsilon_{rf} = \alpha_0 \varepsilon_r$ ([15, 16]). Indeed, the increasing in capacity is the consequence of micro-structure, not of macro-parameters like grains' position or size. Consequently, it may be considered as an intrinsic $BaTiO_3$-ceramics characteristic and also doped $BaTiO_3$-ceramics.

Regarding the energy aspect, the part of energy stored in the grain-grain contact micro-capacity is given by

$$E_{inter}(t) = \frac{1}{2} \alpha_0 \varepsilon_r \varepsilon_0 \frac{v(t)^2}{d} A = \frac{1}{2} C_f v(t)^2. \qquad (9)$$

In the above formula, the distance d is the thickness of contact intergranular zone, while $v(t)$ is the potential difference between two neighbour grains.

Consider the domain U of ceramics material containing N grains ($N \geq 2$). The energy density in U, $\eta_E(U)$, is given by

$$\eta_E(U) = \frac{E(t)}{vol(U)},$$

provided the $E(t)$ denoting the total energy in the domain U, having the volume $vol(U)$. In case that every grain is in contact with four grains

$$N_0 = \frac{3\sqrt{2}}{4} 3^{3/4} .$$

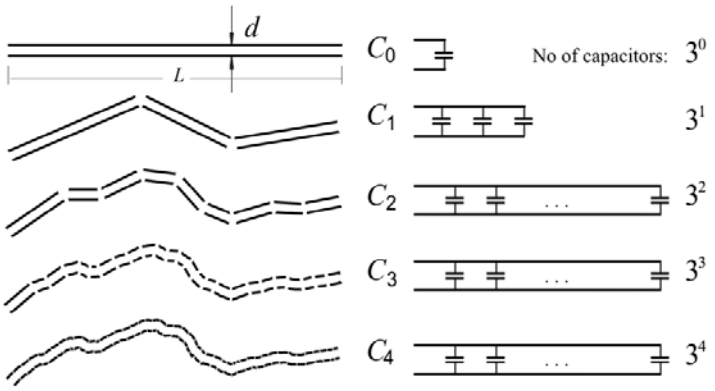

Figure 14. The constructive way is used to explain fractal character of an intergranular micro capacitor grain surfaces

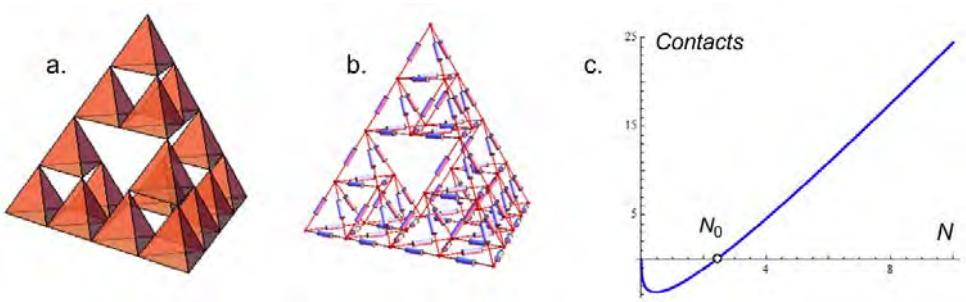

Figure 15. Model of grain cluster forming the pyramid of Sierpinski (a), with intergranular contacts (b) and number of intergranular contacts

5. TEMPERATURE INVOLVEMENT

Arguing about the crystal surface „natural roughness“ as macroscopic steps collection on the arbitrary section surface of the crystal plane section, the authors of [30] quote an observation Frenkel [31] had come forward with, that this roughness does not coincide with the crystal faces atomic roughness, with small surface energy, which can occur as a thermal fluctuations consequence at high temperatures. This temperature consideration illustrates the impact on dynamical processes inside the ceramics body. Such impact generates a motion inside the ceramics crystals in the Fermi gas form, containing different particles such as electrons (Bloch wave), atoms, atomic nuclei etc. In essence, this motion has a Brownian character and imposes necessity of introducing the third fractality factor–factor of movements, α_M $(0<\alpha_M<1)$. Our hypothesis ([25]) is that $BaTiO_3$-ceramics working temperature must be influenced by these three fractality factors, making correction of „theoretic" temperature as

$$T_f = \alpha T, \tag{10}$$

where α is a fractal corrective factor. It is natural that all three factors α_S, α_P, and α_M, influences

$$\alpha = \Phi(\alpha_s, \alpha_P, \alpha_M) \tag{11}$$

The argument for this expectation hides in the fact that geometrically irregular motion of huge particles number has to unleash an extra energy to the system. In other words, fractality of the system represented by three factors α_S, α_P, and α_M should increase overall energy of the system, and this increment must be subtracted from input energy which is in fact, an input thermal energy denoted by T. In other words, $T_f = T - \triangle T$ and since it follows from (10) that $\alpha = \frac{T_f}{T} = \frac{T-\triangle T}{T}$, it gives $0 < \alpha = 1 - \triangle T / T < 1$.

The nature of the function in (11) is unknown by now, but at the first moment, the linear approximation will suffice,

$$\Phi(\alpha_s, \alpha_P, \alpha_M) = u\alpha_s + v\alpha_P + w\alpha_M,$$

where $u, v, w > 0$ are real coefficients satisfying $u + v + w = 1$.

Back to formula (9) gives us a hint of alpha correction embodied in the corrective coefficient α_0. On the other hand, in formula (10) another corrective coefficient, this time corrects the temperature. To find a connection between α_0 and α,, consider the Curie-Weiss law, giving temperature dependence dielectric constants of $BaTiO_3$-ceramics grains' contact zone

$$\varepsilon_r(T) = \frac{C_c}{T - T_S} \tag{12}$$

where *Ts* is the Curie temperature and Cc is Currie constant. If ε_r is corrected to gain the value $\alpha_0\varepsilon_r$, then from (10) and (12) it follows $\alpha_0\varepsilon_r = C_c / (\alpha T - T_S)$. After elimination of Currie constant *Cc* using (12), one gets

$$\alpha = \frac{1}{\alpha_0} + \left(1 - \frac{1}{\alpha_0}\right)\frac{T_C}{T}, \text{ and reversely } \alpha_0 = \frac{T - T_C}{\alpha T - Tc}, \tag{13}$$

which are the formulas and α_0 with temperature *T*. Figure 17 visualizes the relationship between α and α_0, where the natural range for both α and α_0, are deliberately extended for better insight.

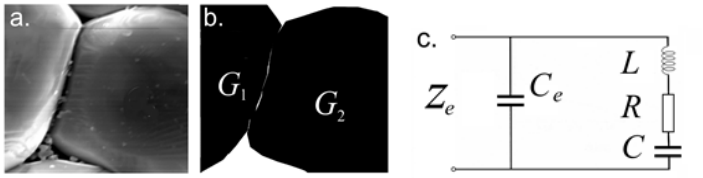

Figure 16. a.Two grains of BaTiO3-ceramics doped with 0.1% of Ho2O3, sintered at 1350 ℃. b. Shematic illustration of G1-G2 contact. c. Equivalent micro-impedance without α-correction

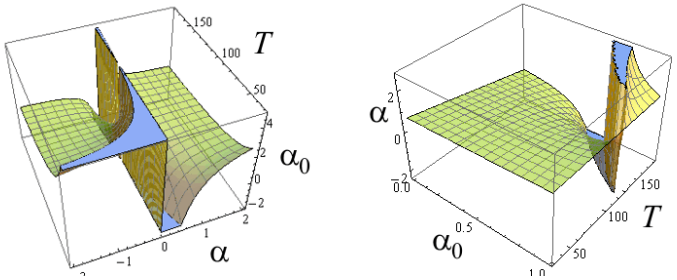

Figure 17. Figure 7. Left. C_e=0.1; C=0.01; L=0.001; Right. C_e =0.01; R=1; L=0.001;{α, 0, 1}, {f, 1, 80}

6. CONCLUSION

In this article the doped BaTiO3-ceramics fractality on some energetic consequences are investigated. It is not new that ceramics, from powder phase through all sintering phases, exhibits fractal structure and microstructure posing a basis for ceramics' dielectric, ferroelectric, PTCR and piezoelectric properties. A special stress is put on the relation of ceramics microstructure and integral micro capacity. The connection between energy storage and energy harvesting from high concentration of micro capacitors using energy density model, has fractal dimension of the ceramics material as a parameter. Based on previous investigations (papers [9-10, 12-29]) where some of $BaTiO_3$-ceramics elements fractality and also for doped $BaTiO_3$-ceramics were established, a new approach to intergranular capacity is developed. Also, the relationship between the size of the contact area and its fractal dimension is formulated. It is shown that the fractal form of an intergranular contact zone may be presented as a chain of micro-capacitors forming one bigger capacitor. It is shown how the capacity increases as the complexity of contact zone increases. The alpha correction of intergranular capacity is introduced to reflect an increase in capacity due fractal character of intergranular contact. The correction factor is $\alpha_0 > 1$. Next, the pores geometry in $BaTiO_3$-ceramics material is investigated with conclusion that all pores collection in ceramic body is a fractal object too. The porosity behavior is studied in all of sintering process three phases, Frenkel, Scherer and Mackenzie-Shuttleworth, and corresponding formulas for box-dimension of pores are established. A third source of fractality, except intergranular surface geometry quantified by the factor α_S and pore system that yields factor α_P, in $BaTiO_3$-ceramics is interior movements of different particles, subatomic, atomic, molecular etc. Due to its Brownian nature, it also has fractal character defined by the third factor α_M. These three factors α_S, α_P, and α_M, are arguments of a functional parameter α that represents all of them. The relationship between α and α_0 is established and two different models of grain clustering is considered. As it is shown in [25] the four grains-tetrahedral, diminishes the total capacity of four intergranular contacts by 40% while the eight grains-cubic connection increases it by 20%. This shows dependence of the inner energetic capacity of ceramic materials on its fractality, which promotes fractal structures as a serious capacity in storage of energy.

7. REFERENCES

[1] V. V. Mitić, Lj. Kocić, M. Miljković, I. Petković, *Fractals and $BaTiO_3$-Ceramic Microstructure Analysis*, Mickrohim. Acta, [Suppl.] 15 (1998) 365−369.

[2] Lj. M. Kocić, V. V. Mitić, M. M. Ristić, *Stereological Models Simulation of $BaTiO_3$-Ceramics Grains*, J. Materials Synthesis and Processing, Vol. 6−5 (1998) 339−344.

[3] B. Mandelbrot, *The Fractal Geometry of Nature* (3ed.), W. H. Freeman, San Francisco 1983.

[4] B. Mandelbrot, *Les objets fractals, forme, hasard et dimension*, Flammarion, Paris 1975.

[5] M. Barnsley, *Fractals Everywhere*, Academic Press, 1988.

[6] B. H. Kaye, *A Random Walk Through Fractal Dimensions*, Wiley-VCH 1994.

[7] A. Naman, *Mechanical Property and Fractal Dimension Determination in Li2O*2SiO2 Glass-ceramics*, University of Florida, 1994.

[8] N. M. Brown, *The Fractal Dances of Nature*, Penn State News, November 19, 2014.

[9] V. V. Mitić, Lj. M. Kocić, M. M. Ristić, *The Interrelations between Fractal and Electrical Properties of BaTiO3-Ceramics*, The American Ceramic Society 99th Annual Meeting and Exposition, Cincinnati, Ohio 1997, 199.

[10] V. V. Mitić, Lj. M. Kocić, M. Miljković, I. Petković, *Fractals and $BaTiO_3$-Ceramic Microstructure Analysis*, Mikrochim. Acta, Suppl. 15 (1998) 365−369.

[11] B. M. Smirnov, *Physics of fractal clusters*, Contemporary problems in Physics, Nauka, Moscow 1991.

[12] V. V. Mitić, Lj. M. Kocić, Z. I. Mitrović, M. M. Ristić, *$BaTiO_3$-Ceramics Microstructure Controlled Using Fractal Methods*, Abstract Book of 100th Annual Meeting and Exposition of the American Ceramic Society, May 3-6, 1998, 190.

[13] P. Petković, V. V. Mitić, Lj. Kocić, *Contribution to $BaTiO_3$-Ceramics Structure Analysis by Using Fractals*, Folia Anatomica, Vol. 26−1 (1998) 67−69.

[14] V. V. Mitić, Lj. M. Kocić, I. Z. Mitrović, M. M. Ristić, *Shapes and Grains Structures Stochastic Modelling in Ceramics*, Proc. of S4G - International Conference on Stereology, Spatial Statistics and Stochastic Geometry, Prague 1999, 209−215.

[15] V. V. Mitić, Lj. Kocić, Z. I. Mitrović, *Application of fractals in the model of intergranular*

impedance of $BaTiO_3$ ceramic materials, Triade Synthesis-Structure-Properties-Basis of the new material technologies, Book of Abstracts, Belgrade 1999, 65−66.

[16] V. V. Mitić, Lj. Kocić, Z. I. Mitrović, *Fractals and $BaTiO_3$-Ceramics Intergranular Impedance*, Gordon Research Conference: Ceramics, Solid State Studies in, Kimball Union Academy, Meriden, New Hampshire, 1999, 54.

[17] V. V. Mitić, V. Paunović, J. Purenović, S. Janković, L. Kočić, I. Antolović, and D. Rančić, *The Contribution of Fractal Nature to $BaTiO_3$-Ceramics Microstructure Analysis*, Ceramics International, Vol. 38−2 (2012) 1295−1301.

[18] V. V. Mitić, V. Paunović, J. Purenović, Lj. Kocić, V. Pavlović, *Processing parameters influence on $BaTiO_3$-ceramics fractal microstructure and dielectric characteristics*, Advances in Applied Ceramics: Structural, Functional and Bioceramics, Vol 111−5&6 (2012) 360−366.

[19] V. Paunović, V. V. Mitić, M. Miljković, Lj. Živković, *Ho_2O_3 Additive Effects on $BaTiO_3$ Ceramics Microstructure and Dielectric Properties*, Science of Sintering, Vol. 44−2 (2012) 223−233.

[20] V. V. Mitić, V. Paunović, S. Janković, V. Pavlović, I. Antolović, D. Rančić, *Electronic ceramic structure within the Voronoi cells model and microstructure fractals contacts surfaces new frontier applications*, Science of Sintering, Vol. 45−2 (2013) 223−232.

[21] V. V. Mitic, V. Paunovic, Lj. Kočić, S. Janković, V. Pavlović, *Microelectronics iniaturization and fractal electronic frontiers*, The Serbian Ceramic Society Conference „Advanced Ceramics and Application II“, SASA, Belgrade, Serbia 2013, 15 (Invited).

[22] V. V. Mitić, V. Paunović, Lj. Kocić, *Dielectric Properties of $BaTiO_3$ Ceramics and Curie-Weiss and Modified Curie-Weiss Affected by Fractal Morphology*, in: Advanced Processing and Manufacturing Technologies for Nanostructured and Multifunctional Materials (T. Ohji, M. Singh and S. Mathur eds.), Ceramic Engineering and Science Proceedings, Vol. 35−6 (2014) 123−133.

[23] V. V. Mitić, V. Paunović, Lj. Kocić, *Dielectric Properties Of $Batio_3$ Ceramics And Curie Weiss And Modified Curie-Weiss Affected By Fractal Morphology*, in: Advanced Processing and Manyfacturing Technologies for Nanostructured and Multifunctional Materials (T. Ohji, M. Singh and S. Mathur eds.), Ceramic Engineering and Science Proceedings, Vol. 35−6, 2014, 123−133.

[24] V.V. Mitić, V. Paunović, Lj. Kocić, S. Janković, V. Litovski, *$BaTiO_3$-Ceramics Microstructures New Fractal Frontiers*, 13th Ceramics Congress, CIMTEC 2014, Montecatini, Italy 2014, CJ-1.L14 .

[25] V. V.Mitić, V. Paunović, Lj. Kocić, *Fractal Approach to $BaTiO_3$-Ceramics Micro-Impedances*, Cer. Int., Vol. 41−5 (2015) 6566–6574

[26] V. Paunović, M. Marjanović, M. Đorđević, V. V. Mitić, Lj. Kocić, *Electrical Characteristics of Nb Doped $BaTiO_3$ Ceramics*, Proceedings of the III Advanced Ceramics and Applications Conference, Belgrade (Serbia) 2014, Atlantis Press 2016, 143−158.

[27] D. Petković, V. V. Mitić, Lj. Kocić, *Adaptive Neuro-Fuzzy Optimization of Wind Farm Project Investment Under Wake Effect*, Proceedings of the III Advanced Ceramics and Applications Conference, Belgrade (Serbia) 2014, Atlantis Press 2016, 265−282.

[28] V. V. Mitić, D. Petković, Lj. Kocić, *TRIZ Creativity Approach to the Design of an Innovative Wind Turbine System*, Proceedings of the III Advanced Ceramics and Applications Conference, Belgrade (Serbia) 2014, Atlantis Press 2016, 283−306.

[29] F. Bastić, D. Sirmić, V. V. Mitić, Lj. Kocić, V. Paunović, S. Janković, M. Miljković, *The Sintering Temperature and the Ho_2O_3 Concentration Influence on $BaTiO_3$ - Ceramics Microstructure Fractal Nature*, Proceedings of the III Advanced Ceramics and Applications Conference, Belgrade (Serbia) 2014, Atlantis Press 2016, 307−320.

[30] L. E. Geguzin, N. I. Ovčarenko, *Surface energy and processes on the surface of the solid state*, Uspehi F. N., Vol. 76−2 (1962) 283−324.

[31] Ya. I. Frenkel', *On the surface crawling particles in crystals and the natural roughness of natural faces*, JETP 16 (1), 1948.

ꕥ

НАУКА О МАТЕРИЈАЛИМА И ЕНЕРГЕТСКА ФРАКТАЛНА ПРИРОДА НОВЕ ГРАНИЦЕ

Сажетак: Модерна наука о материјалима суочава се са веома важним приоритетима будућих нових граница што отвара нове правце ка знању о вишим и дубљим структурама чак до нано нивоа, а због недостатка енергије, према новим и алтернативним изворима енергије. На примјер, у досадашњим истраживањима смо признали

да је природа конфигурације $BaTiO_3$ и остале керамике фрактална на основу три различите појаве. Прво, зрна керамике имају фрактални облик било као контура у попречном пресјеку или као површ. Друго, постоји такозвани „негативни простор“ сачињен од пора и интергрануларног простора. Будући да је крајње комплексан, простор пора игра важну улогу у микроелектроници, микро-капацитету, PTC-у, пиезоелектричним и осталим појавама. Треће, постоји Браунов процес фракталног кретања унутар материјала за вријеме и након синтеринга у форми тока микрочестица: јона, атома и електрона. Овдје сусрећемо интригантан задатак Кобловог модела, са већ проширеном и генерализованом геометријом. Ова три фактора у комбинацији праве од микроелектронског окружења јединствену електро-статичку/динамичну комбинацију. Нагласак је при овоме стављен на интергрануларни микрокапацитет и супер микро-кондензаторе у функцији већег прикупљања енергије из спољашњег извора и складиштења енергије. Пажња је посвећена компонентама које утичу на цјелокупну расподјелу импеданси. Конструктивна фрактална теорија омогућава прихватање микро-кондензатора са фракталним електродама. Метод се заснива на итеративном процесу интерполације који је компатибилан са моделом самих зрна. Интергрануларна пермеабилност се разматра у функцији температуре као основног термодинамског параметра.

Кључне ријечи: $BaTiO_3$-керамика, фрактали, микроструктура, микроимпедансе.